ELECTRONIC SUPPLEMENTARY INFORMATION

For

Self-Assembly of Unprecedent [8+12] Copper Metallamacrocycle-Based 3D MOFs

Zhouqing Xu,[a,b] Qiang Wang,[b] Huijun Li,[a] Wei Meng,[a] Yi Han,[a] Hongwei Hou*[a] and Yaoting Fan[a]

[a] Department of Chemistry, Zhengzhou University, Henan 450052, P. R. China.
[b] Department of Physical Chemistry, Henan Polytechnic University, Jiao Zuo 454000, P. R. China.

* To whom correspondence should be addressed: Pro. H.-W. Hou, E-mail: houhongw@zzu.edu.cn. Fax: (86) 0371-67761744;

1. Materials and methods

All chemicals were obtained from commercial sources and used as received without purification except the anhydrous solvents.

IR data were recorded on a BRUKER TENSOR 27 spectrophotometer with KBr pellets in the region of 400–4000 cm^{-1}. Elemental analyses (C, H and N) were carried out on a Flash EA 1112 elemental analyzer. Themogravimetric analyses were carried out with a NETZSCH STA 409 unit at a heating rate of 10 °C min^{-1} under a nitrogen atmosphere. X-ray powder diffraction measurements were recorded on a Philips X'pert PRO SUPER X-ray diffractometer using graphite monochromatized CuKα radiation (λ = 1.541874 Å).

2. Single Crystal X-ray Diffraction Analyses

Single-crystal X-ray diffraction data was collected from a turquoise rhombus crystal for **1** and a blue block for **2**, respectively, sealed in a capillary at room temperature (296 K) on a Bruker SMART Apex II CCD-based X-ray diffractometer system equipped with graphite-monochromated Mo-Ka radiation generated from a sealed tube (0.71073 Å). The Bruker SMART[1] program was used for analysis of the data collection, and SAINT[2] was used for the cell refinement, and reduction. Absorption corrections were applied using SADABS[3]. All of the structures were solved by direct methods and refined to convergence by least squares method on F^2 using the SHELXTL[4] software suit. Non-hydrogen atoms except some terminal solvent molecules and solvated water molecules were refined with anisotropic displacement parameters during the final cycles. All hydrogen except for solvated water molecules were placed in calculated positions and refined by applying a riding model; it was not possible to find the hydrogen atoms of the water molecules. The distances and angles in the terminal DMF, MeOH and water molecules for **1** and DMSO and MeOH molecules for **2**, respectively, were restrained using DFIX, SIMU, DELU and ISOR during the leastsquares refinement because of poor geometry. In structures with voids, attempts to locate and model the highly disordered solvent

molecules in the voids were unsuccessful. Therefore, the SQUEEZE routine of PLATON[5] was used to remove the diffraction contribution from these solvents to produce a set of solvent-free diffraction intensities. The large volume fraction of disordered solvents was calculated by PALTON SOLV CALC[5] to 12450.8 Å^3 and 4833.3 Å^3 which corresponds to 46.0% and 35.9% of the unit cell volume for **1** and **2**, respectively.

3. Synthesis procedures

3.1 Synthesis of $\{[Cu_4(pbt)_2(SO_4)_2(DMF)_2(CH_3OH)]\cdot 7H_2O\cdot DMF\}_n$ (**1**)

A MeOH solution of $CuSO_4\cdot 5H_2O$ (9.6 mg in 3 mL) was carefully layered onto a N,N-dimethylformamide (DMF) solution of H_2pbt (6.3 mg in 3 mL). After the solution was allowed to stand for about 7 days, the turquoise rhombus crystals formed were isolated in 73% yield by filtration. Elemental analysis data calcd for $\{[Cu_4(pbt)_2(SO_4)_2(DMF)_2(CH_3OH)]\cdot 7H_2O\cdot DMF\}_n$ (**1**) ($C_{28}H_{49}N_{17}S_2Cu_4O_{19}$) : C:26.98, H:3.96, N:19.10; found C 26.12, H 3.03, N 20.14. IR (KBr, cm–1): 3440, 1652, 1616, 1570, 1463, 1434, 1312, 1114, 1042, 796, 754, 718, 647, 594.

3.2 Synthesis of $\{[Cu_2(pbt)(SO_4)(DMSO)(CH_3OH)_2]\cdot 5H_2O\cdot CH_3OH\}_n$ (**2**)

Complex 2 was synthesized adopting a procedure similar to that for 1, except that the solvent DMF was replaced by dimethylsulfoxide (DMSO). Blue rectangular crystals of **2** were obtained in 46% yield. Elemental analysis data calcd for $\{[Cu_2(pbt)(SO_4)(DMSO)(CH_3OH)_2]\cdot 5H_2O\cdot CH_3OH\}_n$ (**2**) ($Cu_2C_{14}H_{33}N_7O_{13}S_2$): C:24.07, H:4.76, N:14.03; found C:23.63, H:3.88, N:15.88, IR (KBr, cm–1): 3339, 1616, 1570, 1462, 1434, 1313, 1196, 1116, 1030, 951, 795, 754, 718, 648, 594.

Compounds **1** and **2** are all insoluble in water and common organic solvents but efflorescent in air. The similarity between the PXRD pattern of the as-synthesized bulk crystals and that simulated from the single-crystal structure of as synthesized indicates that the single-crystal structure represents the bulk crystal samples. They were characterized by elemental microanalysis, IR spectroscopy, single-crystal X-ray diffraction, powder X-ray diffraction (PXRD) Figure (Figure S11, S12) and thermal gravimetric analysis (TGA) (Figure S13).

Note: the solvent molecules for **1** and **2** were estimated from the result of PLATON

– SQUEEZE, the TG data, and the data of elemental analyses, and were included in the molecular formula directly.

4. Magnetic properties measurement

Magnetic susceptibility measurements were carried out for **1** and **2** in a temperature range from 2.8 to 300K in a 2000 Oe applied field. The magnetic properties of complex **1** and **2** as $\chi_m T$ vs. T and χ_m^{-1} vs. T plot (χ_m is the molar magnetic susceptibility) are shown in Figure S9 and Figure S10. As shown in Figure S9, the $\chi_m T$ value at room temperature in **1** is 1.33 cm^3 K mol^{-1}, which is lower than the spin-only value of 1.5 cm^3 K mol^{-1} expected for four magnetically uncoupled Cu(II) ions (S = 1/2), and the $\chi_m T$ values decrease first slowly and then rapidly, reaching a maximum of 0.24 cm^3 K mol^{-1} at around 2.8 K. This behavior suggests the existence of antiferromagnetic exchange behavior. The $\chi_m T$ value for **2** at 300 K is 0.77 cm^3 K mol^{-1}, significantly lower than the spin-only value of 0.75 cm^3 K mol^{-1} expected for two magnetically isolated Cu(II) ions (S = 1/2). By decreasing the temperature, the $\chi_m T$ gradually decreases reaching 0.0449 cm^3 K mol^{-1} at 2.7 K, suggesting a dominant antiferromagnetic interaction between the Cu(II) centers. The abrupt increasing of XmT at lower temperature indicates that a small amount of paramagnetic impurity exists, which is a common phenomena in this type of system. Similar explanation has been reported by G. Arom.[6]

5. Complex 1 catalyzes Oxidative Coupling of Phenylacetylene and 2-Oxazolidinone

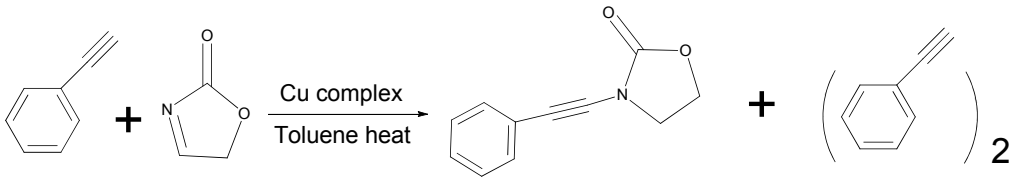

1-ethynylbenzene oxazolidin-2-one 3-(2-phenylethynyl)oxazolidin-2-one 1,4-diphenylbuta-1,3-diyne

In a 25 ml three-neck round-bottom flask equipped with a stir-bar, crystal **1** (0.02 mmol, 22.1 mg) or crystal **2** (0.01 mmol, 13.4 mg), 2-oxazolidinone (0.5 mmol, 43 mg) and Na_2CO_3 (0.2 mmol, 21.2 mg) and 4.0 ml dry toluene were added to the reaction flask via a syringe. The reaction flask was purged with oxygen gas for 15

minutes. A balloon filled with oxygen gas was connected to the reaction flask via a needle. The flask was placed in an oil-bath and heated to 75 °C. A solution of phenylacetylene (0.2 mmol, 20.2 mg) in 2.0 ml dry toluene was added to the flask over 4 h by using a syringe pump. After the addition of phenylacetylene/toluene solution, the reaction mixture was allowed to stir at 75 ºC for another 4 h and then cooled to room temperature. After the crude mixture was concentrated under vacuum, the reaction mixture was purified by flash chromatography on silica gel with hexanes/ethyl acetate (7/3) to yield the principal product 3-(2-phenylethynyl)oxazolidin-2-one (29.2 mg, 78% yield for complex **1** and 24.7 mg, 66% yield for complex **2**). Colorless solid 3-(2-phenylethynyl)-oxazolidin-2-one was characterized by IR: 3423(m), 2965(m), 2911(m), 2265(s), 1758(s), 1472(m), 1423(s), 1218(s), 1163(m), 1091(m), 1023(m), 748(s), 690(s), and ^{1}HNMR: δ 7.46-7.43 (m, 2H), 7.32-7.29 (m, 3H), 4.50-4.45 (m, 2H), 4.02-3.97 (m, 2H).

6. Supporting scheme, tables and figures

Scheme 1: The two binding modes of ligand in **1** and **2**. (a) A ligand bridges three metal centers; (b) A ligand bridges four metal centers.

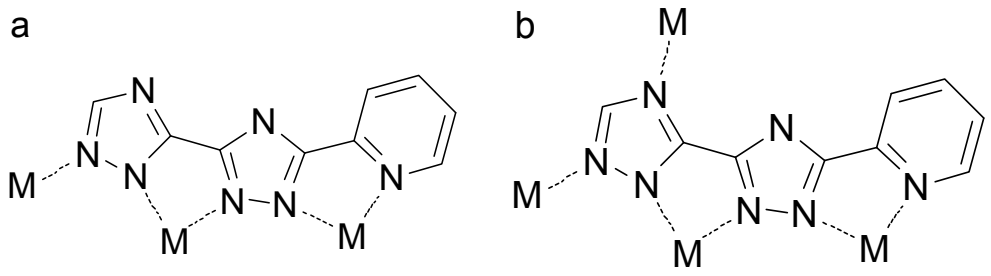

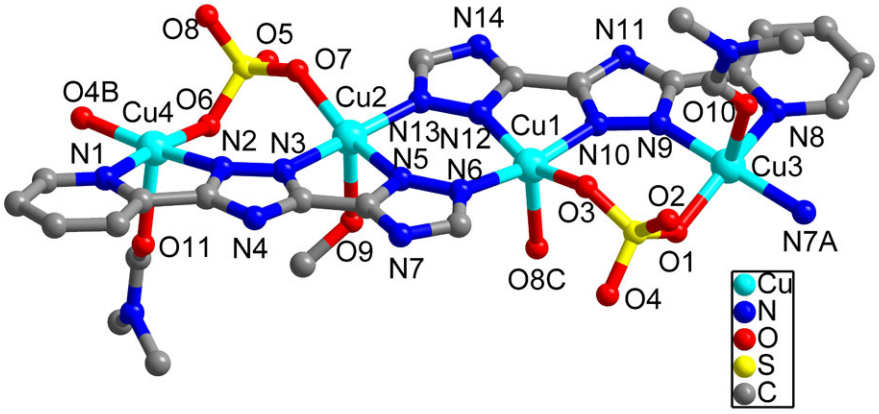

Figure S1. The coordination enviornment of Cu(II) ions in **1**. Symmetry code: A: 0.33333+y, 0.66667-x+y, 0.6667-z; B: 0.66667-x+y, 0.33333-x, 0.33333+z; C: 0.33333-y, -0.33333+x-y, -0.33333+z.

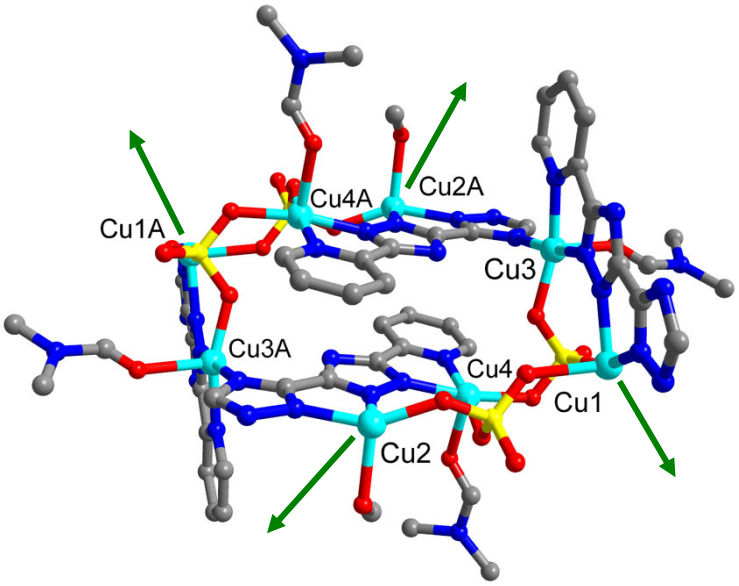

Figure S2. View of the chair-shaped octanuclear macrocycle builing block. Symmetry code: A: -x, 1-y, -z.

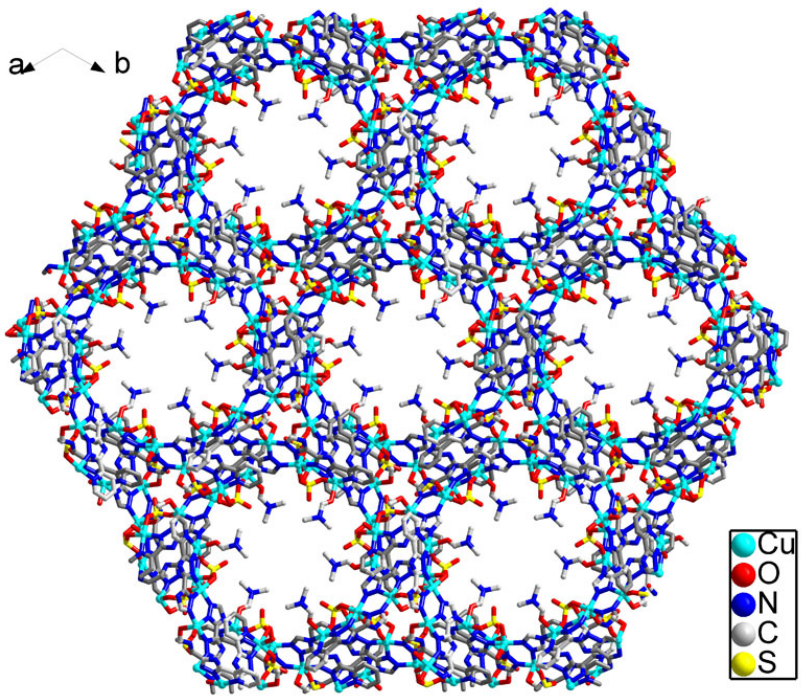

Figure S3. View of the channels and packing designsketch of **1** along the *c* axis. MeOH molecules and discrete solvent molecules have been omitted for clarity.

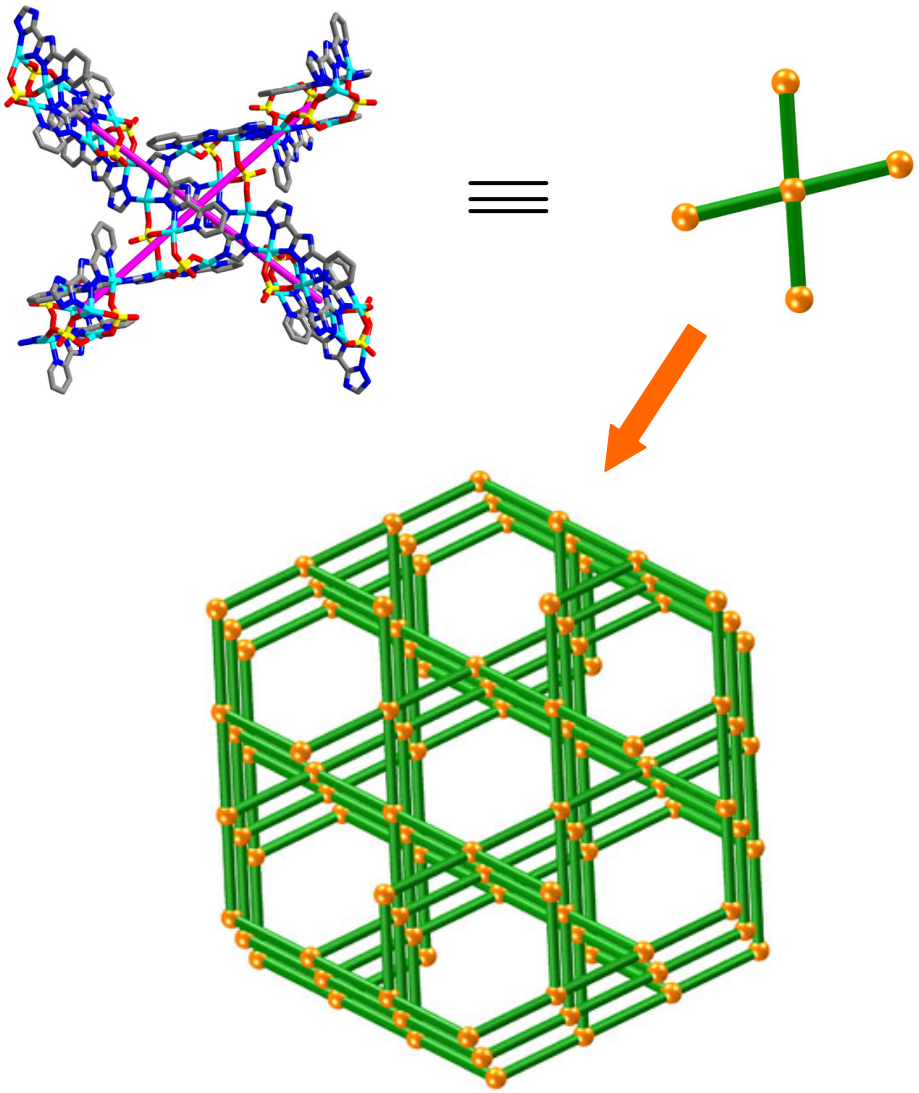

Figure S4. Schematic view of the 4-connected net in **1**.

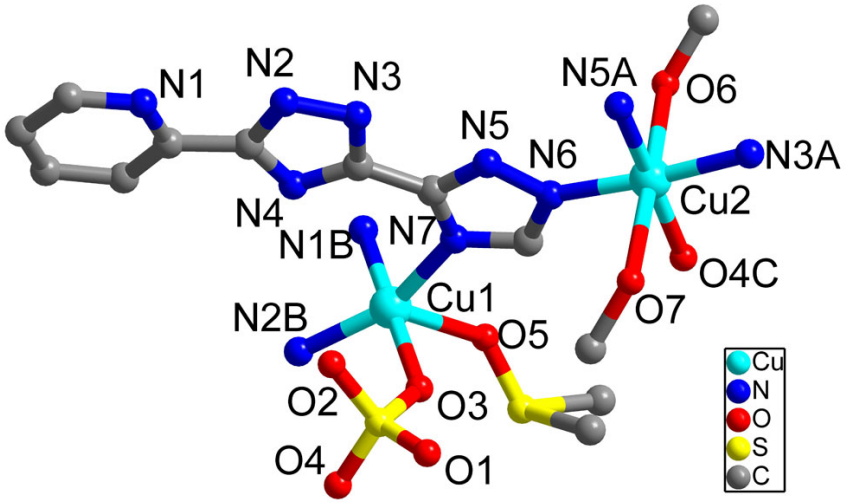

Figure S5. The coordination of environment of Cu(II) ions in **2**. Symmetry codes: A: 1-x, -y, 2-z; B: 1.33333-x+y, 0.66667-x, -0.33333+z; C: 0.33333+y, 0.66667-x+y, 1.66667-z.

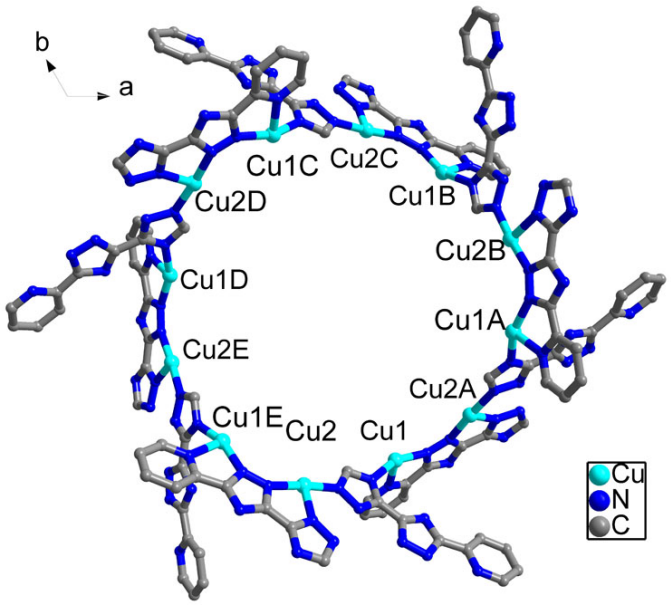

Figure S6. View of the dodecameric copper macrocycle building block in **2**. Terminal solvent molecules and SO_4^{2-} anions have been omitted for clarity. Symmetry code: A: 0.33333+x-y, -0.33333+x, 1.66667-z; B: 1-y, x-y, z; C: 1.33333-x, 0.66667-y, 1.66667-z; D: 1-x+y, 1-x, z; E: 0.33333+y, -0.33333+x, 1.66667-z.

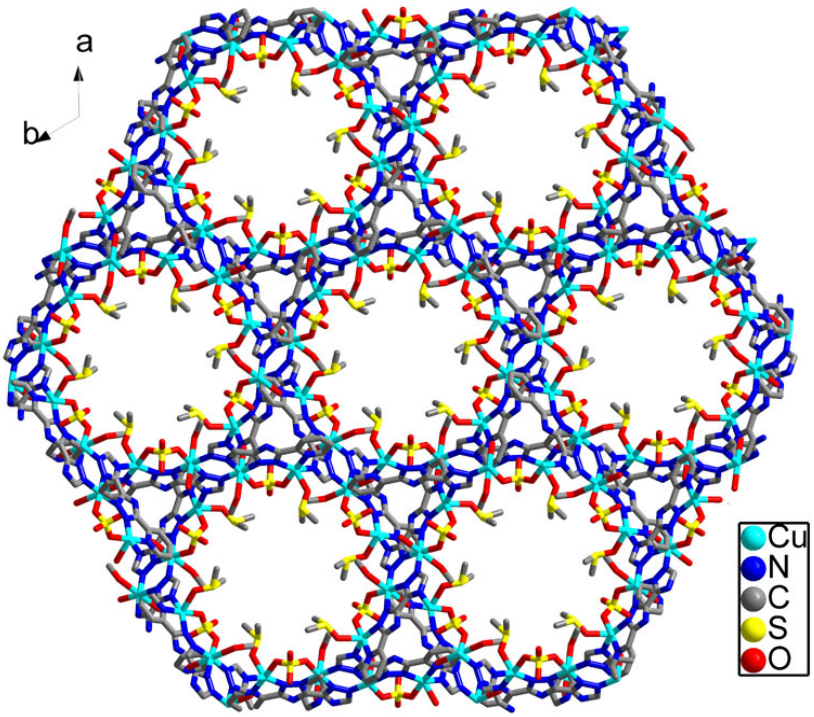

Figure S7. View of the channels and packing designsketch of **2** along the *c* axis. MeOH molecules and discrete solvent molecules have been omitted for clarity.

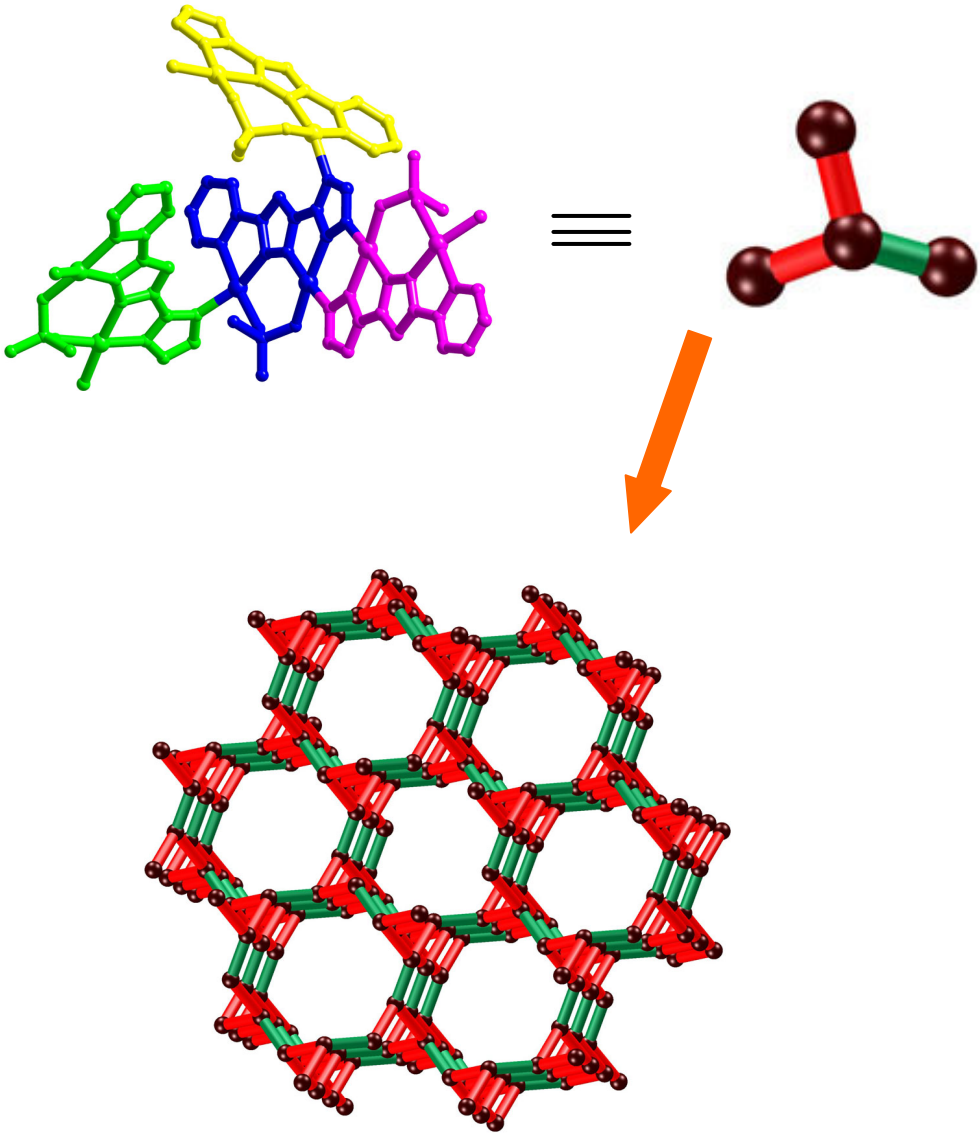

Figure S8. A schematic view of the 3-connected net of **2**.

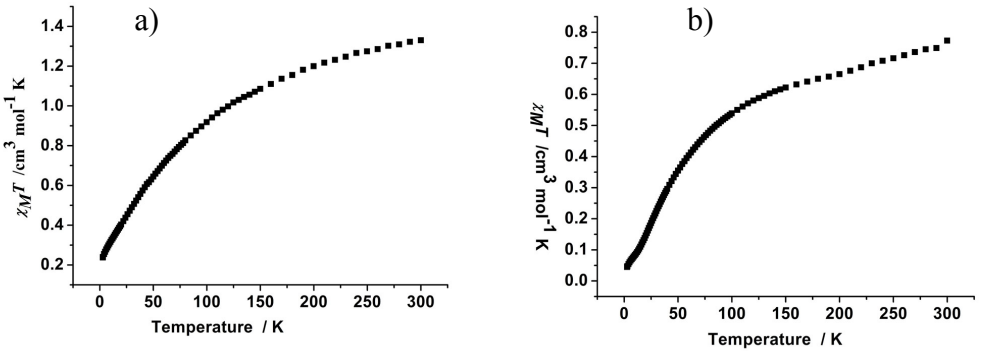

Figure S9. The $\chi_m T$ versus T plots for **1** (a) and **2** (b).

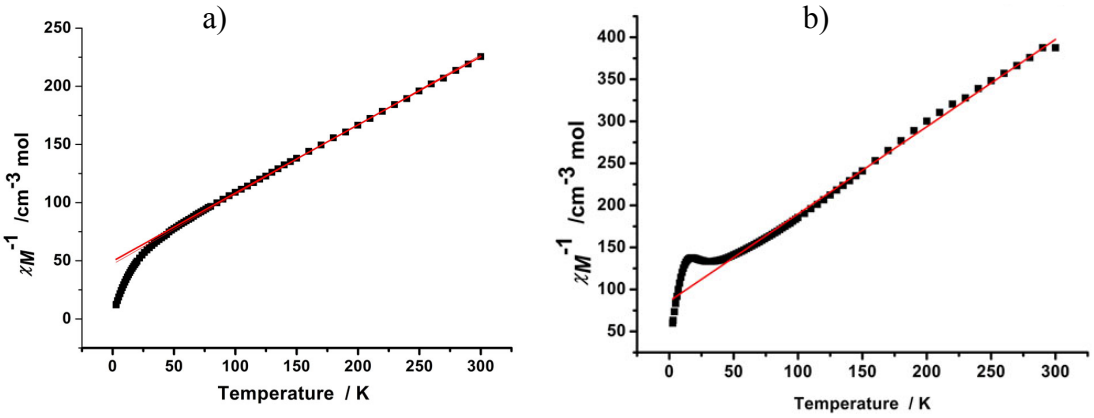

Figure S10. The χ_m^{-1} versus T plots for **1** (a) and **2** (b).

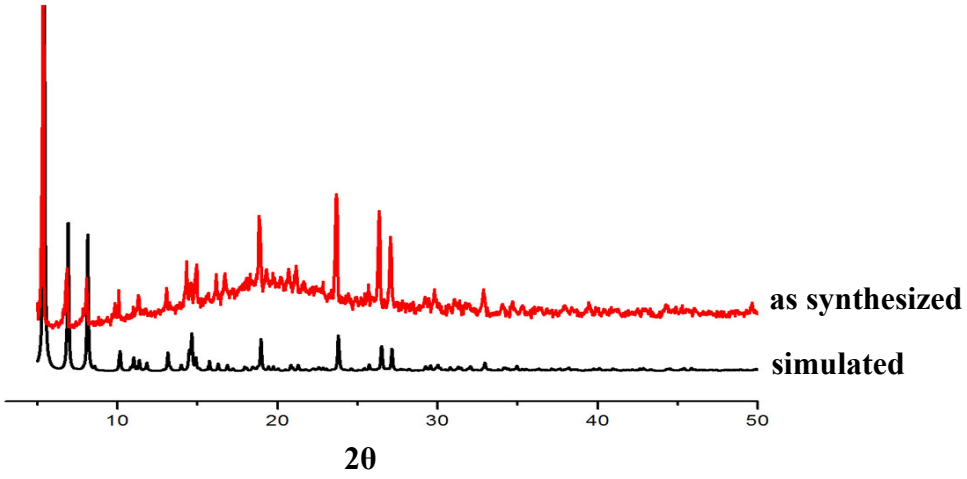

Figure S11. Experimental (red) and simulated (black) powder X-Ray diffraction patterns for **1**.

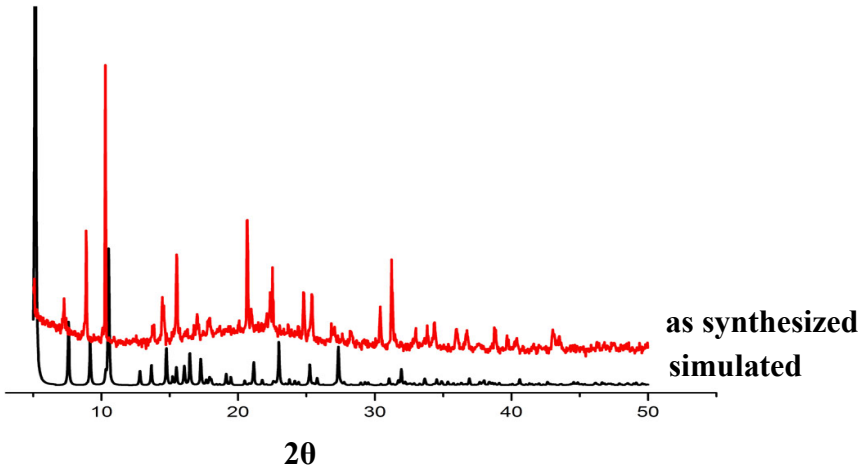

Figure S12. Experimental (red) and simulated (black) powder X-Ray diffraction patterns for **2**.

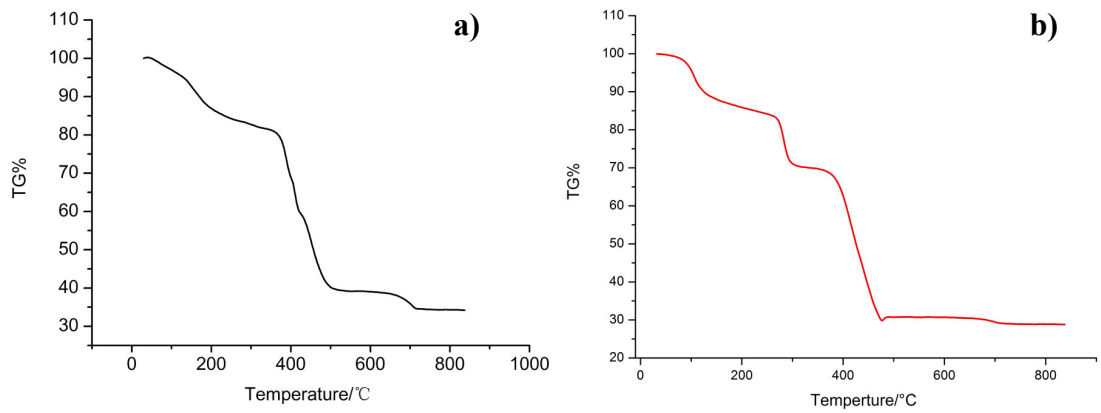

Figure S13. TG curves of **1** (a) and **2** (b).

Table 1. Crystal data and structure refinement details for **1** and **2**.

	complex-**1**	complex -**2**
Formula	$C_{28}H_{49}Cu_4N_{17}O_{19}S_2$	$C_{14}H_{33}Cu_2N_7O_{13}S_2$
Fw	1246.12	698.67
temp/K	296(2)	296(2)
Wavelength (Å)	0.71073	0.71073
crystal system	trigonal	trigonal
space group	*R*-3	*R*-3
a (Å)	41.3528(18)	34.4325(12)
b (Å)	41.3528(18)	34.4325(12)
c (Å)	18.2765(15)	13.0911(9)
α/deg	90	90
β/deg	90	90
γ/deg	120	120
V (Å^3)	27067(3)	13441.4(11)
Z	18	18
D_c (mg·m^{-3})	1.376	1.554
Theta range	1.25 to 28.25	1.18 to 25.49
Limiting indices	-52<=h<=54 -54<=k<=40 -20<=l<=24	-33<=h<=41 -41<=k<=32 -15<=l<=12
F (000)	11448	6480
rflns collected	58156	24617
unique rflns	14834	5559
R(int)	0.0619	0.0348
GOF on F^2	0.998	1.075
R_1[a] (I>2sigmaI)	0.0552	0.0568
wR2(I>2sigmaI)	0.1523	0.1873
R_1 [a](all data)	0.1004	0.0698
wR2	0.1649	0.1985

[a]$R_1 = \sum ||F_o| - |F_c|| / \sum |F_o|$. $wR_2 = [\sum w(|F_o^2| - |F_c^2|)^2 / \sum w|F_o^2|^2]^{1/2}$.

Table 2. Selected bonds (Å) and angles (deg) for **1**.

Cu(1)-N(6)	1.976(4)	Cu(3)-N(9)	1.959(4)
Cu(1)-O(3)	1.990(4)	Cu(3)-O(1)	1.971(4)
Cu(1)-N(10)	1.997(4)	Cu(3)-N(7)	1.983(4)
Cu(1)-N(12)	2.028(4)	Cu(3)-N(8)	2.074(5)
Cu(1)-O(8)	2.217(4)	Cu(3)-O(10)	2.201(5)
Cu(2)-N(13)	1.926(5)	Cu(4)-O(4)	1.963(4)
Cu(2)-O(7)	1.962(4)	Cu(4)-O(6)	1.965(4)
Cu(2)-N(3)	1.963(4)	Cu(4)-N(2)	1.966(5)
Cu(2)-N(5)	2.051(4)	Cu(4)-N(1)	2.066(5)
Cu(2)-O(9)	2.274(5)	Cu(4)-O(11)	2.250(5)
N(6)-Cu(1)-O(3)	88.95(17)	N(9)-Cu(3)-O(1)	93.05(17)
N(6)-Cu(1)-N(10)	169.42(18)	N(9)-Cu(3)-N(7)	167.5(2)
O(3)-Cu(1)-N(10)	93.06(17)	O(1)-Cu(3)-N(7)	91.90(16)
N(6)-Cu(1)-N(12)	94.59(18)	N(9)-Cu(3)-N(8)	80.09(19)
O(3)-Cu(1)-N(12)	158.34(18)	O(1)-Cu(3)-N(8)	161.0(2)
N(10)-Cu(1)-N(12)	79.81(18)	N(7)-Cu(3)-N(8)	91.61(18)
N(6)-Cu(1)-O(8)	98.84(16)	N(9)-Cu(3)-O(10)	100.1(2)
O(3)-Cu(1)-O(8)	103.07(15)	O(1)-Cu(3)-O(10)	105.1(2)
N(10)-Cu(1)-O(8)	90.83(17)	N(7)-Cu(3)-O(10)	89.64(19)
N(12)-Cu(1)-O(8)	97.50(18)	N(8)-Cu(3)-O(10)	93.6(2)
N(13)-Cu(2)-O(7)	91.07(17)	O(4)-Cu(4)-O(6)	91.65(17)
N(13)-Cu(2)-N(3)	171.5(2)	O(6)-Cu(4)-N(2)	93.35(17)
O(7)-Cu(2)-N(3)	91.59(17)	O(4)-Cu(4)-N(2)	169.98(18)
N(13)-Cu(2)-N(5)	94.19(18)	O(6)-Cu(4)-N(1)	172.67(18)
O(7)-Cu(2)-N(5)	151.14(17)	O(4)-Cu(4)-N(1)	95.56(18)
N(3)-Cu(2)-N(5)	79.67(17)	N(2)-Cu(4)-N(1)	79.74(19)
N(13)-Cu(2)-O(9)	93.1(2)	O(6)-Cu(4)-O(11)	91.2(2)
O(7)-Cu(2)-O(9)	115.09(17)	O(4)-Cu(4)-O(11)	92.9(2)
N(3)-Cu(2)-O(9)	93.11(19)	N(2)-Cu(4)-O(11)	95.6(2)
N(5)-Cu(2)-O(9)	92.97(17)	N(1)-Cu(4)-O(11)	87.1(2)

Symmetry transformations used to generate equivalent atoms:

#1 x-y+1/3,x-1/3,-z+2/3 #2 y+1/3,-x+y+2/3,-z+2/3

#3 -x+y+2/3,-x+1/3,z+1/3 #4 -y+1/3,x-y-1/3,z-1/3

Table 3. Selected bonds (Å) and angles (deg) for **2**.

Cu(1)-O(4)	1.9375(1)	Cu(2)-N(4)	1.9668(1)
Cu(1)-N(2)	1.9754(1)	Cu(2)-N(6)	2.0025(1)
Cu(1)-N(3)	1.9890(1)	Cu(2)-N(5)#2	2.0284(1)
Cu(1)-N(1)	2.0269(1)	Cu(2)-O(6)	2.409(2)
Cu(1)-O(5)	2.2778(1)	Cu(2)-O(7)	2.544(3)
Cu(2)-O(3)#1	1.9261(1)		
O(4)-Cu(1)-N(2)	97.78(5)	O(3)#1-Cu(2)-N(5)#2	171.61(6)
O(4)-Cu(1)-N(3)	89.97(5)	N(4)-Cu(2)-N(5)#2	94.52(5)
N(2)-Cu(1)-N(3)	158.29(6)	N(6)-Cu(2)-N(5)#2	80.13(5)
O(4)-Cu(1)-N(1)	173.62(6)	O(3)#1-Cu(2)-O(6)	93.87(8)
N(2)-Cu(1)-N(1)	80.24(5)	N(4)-Cu(2)-O(6)	88.83(7)
N(3)-Cu(1)-N(1)	94.03(4)	N(6)-Cu(2)-O(6)	90.36(7)
O(4)-Cu(1)-O(5)	89.26(6)	N(5)#2-Cu(2)-O(6)	94.14(7)
N(2)-Cu(1)-O(5)	108.31(5)	O(3)#1-Cu(2)-O(7)	83.53(10)
N(3)-Cu(1)-O(5)	91.97(5)	N(4)-Cu(2)-O(7)	88.92(9)
N(1)-Cu(1)-O(5)	85.65(5)	N(6)-Cu(2)-O(7)	92.12(9)
O(3)#1-Cu(2)-N(4)	88.14(5)	N(5)#2-Cu(2)-O(7)	88.56(8)
O(3)#1-Cu(2)-N(6)	97.33(5)	O(6)-Cu(2)-O(7)	176.1(9)
N(4)-Cu(2)-N(6)	174.51(5)		

Symmetry transformations used to generate equivalent atoms:

#1 y+1/3,-x+y+2/3,-z+5/3 #2 -x+1,-y,-z+2 #3 x-y+1/3,x-1/3

7. References

1 Bruker SMART version 5.625, Area-Detector Software Package; Bruker AXS 1997-2001. Madison, WI, USA.

2 Bruker SAINT+ version 6.04. SAX Area-Detector Integration Program. Bruker AXS 1997-2001. Madison, WI, USA.

3 G. M. Sheldrick, *SADABS 2.05*, University of Göttingen, Germany.

4 Bruker AXS SHELXTL version 6.10. Structure Determination Package. Bruker AXS 2000. Madison, WI, USA.

5 A. L. Spek, PLATON, A Multipurpose Crystallographic Tool, 2008. Utrecht University, Utrecht, The Netherlands.

6 G. Arom, J. Ribas, P. Gamez, O. Roubeau, H. Kooijman, A. L. Spek, S. Teat, E. MacLean, H. Stoeckli-Evans and J. Reedijk, Chem Eur J, 2004, **10**, 6476–6478.